High-voltage transmission electron microscope in situ study on dislocation motion in decagonal Al–Ni–Co single quasicrystals

Martin Bartsch
Max-Planck-Institut für Mikrostrukturphysik, D-06120 Halle (Saale), Germany

Peter Schall[a] and Michael Feuerbacher
Institut für Festkörperforschung, Forschungszentrum Jülich GmbH, D-52425 Jülich, Germany

Ulrich Messerschmidt[b]
Max-Planck-Institut für Mikrostrukturphysik, D-06120 Halle (Saale), Germany

(Received 28 October 2004; accepted 15 March 2005)

Decagonal single quasicrystals of the composition $Al_{70}Ni_{15}Co_{15}$ have been deformed in situ in a high-voltage transmission electron microscope at 730 °C along the 10-fold periodic axis to directly observe the dislocation motion. The deformation is carried by stress-assisted climb of dislocations with periodic Burgers vectors. These dislocations may also glide and move by a combination of glide and climb. Dislocations with Burgers vectors with components in the periodic and quasiperiodic directions probably move under the action of a chemical force. The observations are interpreted by a model established by P. Schall et al. under consideration of the activation parameters of macroscopic deformation and by analogies with the behavior of icosahedral quasicrystals.

I. INTRODUCTION

Quasicrystals are materials with long-range order but without translational symmetry. Despite the lack of translational symmetry, they deform plastically by dislocation processes, as was first shown for icosahedral single quasicrystals by an increase of the dislocation density after plastic deformation[1] and by the direct observation of dislocation motion during in situ deformation experiments in a high-voltage transmission electron microscope (HVTEM).[2] Decagonal quasicrystals are two-dimensional quasicrystals; i.e., they consist of quasiperiodic planes with 10-fold symmetry which are stacked in a periodic way. The first macroscopic deformation studies on decagonal quasicrystals revealed a remarkable plastic anisotropy.[3–7] Plastic deformation data were measured in Al–Ni–Co single quasicrystals at loading axes parallel, perpendicular and inclined by 45° against the 10-fold symmetry axis. The flow stress is lower in the latter case. The d ifference depends on the alloy and its composition. The macroscopic deformation data in the former two cases resemble those of icosahedral quasicrystals. Dislocations in decagonal quasicrystals were first analyzed in Ref. 8 showing Burgers vectors both in periodic direction and within the quasiperiodic plane. Recently, the Burgers vectors of dislocations were determined after plastic deformation with compression axes in the three directions mentioned above.[9] The Burgers vector directions were either parallel to the 10-fold axis (in the periodic direction), perpendicular to it (in a quasiperiodic direction), or mixed with both components. The line directions of all dislocations are preferentially oriented parallel or perpendicular to the periodic axis. In the orientation of the present experiments with the tensile direction parallel to the periodic axis, the habit planes of dislocations with Burgers vectors in the periodic direction are perpendicular to this direction;[10] i.e., these loops are of prismatic character. In this orientation, they do not experience a glide force, only a climb force, so that these dislocations should have moved by pure climb. A second set of dislocations with mixed Burgers vectors may supply the necessary vacancy flux. It has only recently turned out that climb seems to be the dominating mode of dislocation motion also in icosahedral quasicrystals, both by in situ straining experiments in a transmission electron microscope between 700 and 750 °C, where the Burgers vectors and the planes of motion were

[a]Present address: Division of Engineering and Applied Sciences, Harvard University, 9 Oxford Street, Cambridge, MA 02138.
[b]Address all correspondence to this author.
e-mail: um@mpi-halle.de
This author was an editor of this focus issue during the review and decision stage. For the *JMR* policy on review and publication of manuscripts authored by editors, please refer to http://www.mrs.org/publications/jmr/policy.html.
DOI: 10.1557/JMR.2005.0227

determined simultaneously,[11,12] and after macroscopic deformation under hydrostatic pressure at 300 °C.[13] Some of the present authors determined the Burgers vector directions and the planes of deformation bands in specimens deformed macroscopically at temperatures between 487 and 580 °C.[14–16] In these specimens, bands occur with only a climb force and such without any force from the applied load. In these bands, dislocations must have moved by pure climb under the external stress and under a chemical force. In other bands, glide can also have contributed to the dislocation motion.

In the experiments on decagonal quasicrystals published so far, the planes of dislocation motion have not been determined directly. Accordingly, it is the aim of the present paper to directly observe the dislocation motion in such a material during in situ deformation in an HVTEM to contribute to clarify the operating dislocation mechanisms.

II. EXPERIMENTAL

Decagonal single quasicrystals of the composition $Al_{70}Ni_{15}Co_{15}$ in the size range of centimeters were grown by the Bridgman technique. This material is the same as that studied in Refs. 7, 9, and 10. Micro-tensile specimens were prepared for the in situ straining experiments. Slices of about 8 × 2.5 × 0.3 mm were cut by spark erosion with the long axis parallel to the 10-fold symmetry axis and the plane perpendicular to the P2 2-fold axis. Two holes of about 0.6-mm diameter were drilled by spark erosion with a separation of 5 mm for fixing the specimens onto the tensile stage. The slices were carefully ground and polished down to a thickness below about 0.1 mm. The central area was dimpled by a special dimpler producing a wide thin area. Afterwards, the specimens were polished by electrolytic jet polishing in a solution of 1 part of nitric acid in two parts of methanol at −35 °C in two steps. In the first short step the polishing occurred only through an aperture in the central region. In the second step, the edges of the middle of the specimen were also exposed to the jet so that they were thinned, too, to reduce the load necessary for deformation. The thinning was stopped after perforation.

The in situ straining experiments were performed in a special double-tilting high-temperature straining stage for the HVTEM allowing temperatures above 1150 °C.[17] The micro-tensile specimens were fixed to the grips of this stage by tungsten pins. The HVTEM was operated at 1 MeV. The straining was carried out at 730 °C in small load increments. The applied force was measured by a full bridge of semiconducting strain gauges attached to the straining stage allowing a controlled loading and unloading. The changes of the microstructure were recorded on photographic film or by a video system. Three successful experiments were carried out.

III. RESULTS

A. Imaging conditions

According to Ref. 9, deformed decagonal Al–Ni–Co quasicrystals show three different types of dislocations: dislocations with a Burgers vector in the 10-fold periodic direction, with a Burgers vector with a parallel component in the quasiperiodic plane, and with a mixed Burgers vector having components both in the periodic and a quasiperiodic direction. Special representatives of these Burgers vectors are B(1) = [00001] (in the notation of Steurer et al.[18]) for the periodic, B(2) = $[\bar{1}0010]$ and B(3) = $[\bar{1}\bar{1}010]$ for the quasiperiodic and B(4) = $[\bar{1}/5\ \bar{1}/5\ \bar{1}/5\ \bar{1}/5\ 1/2]$ for the mixed dislocation.

The characteristic microstructure during in situ deformation is shown in Fig. 1(a). Figure 1(b) presents a

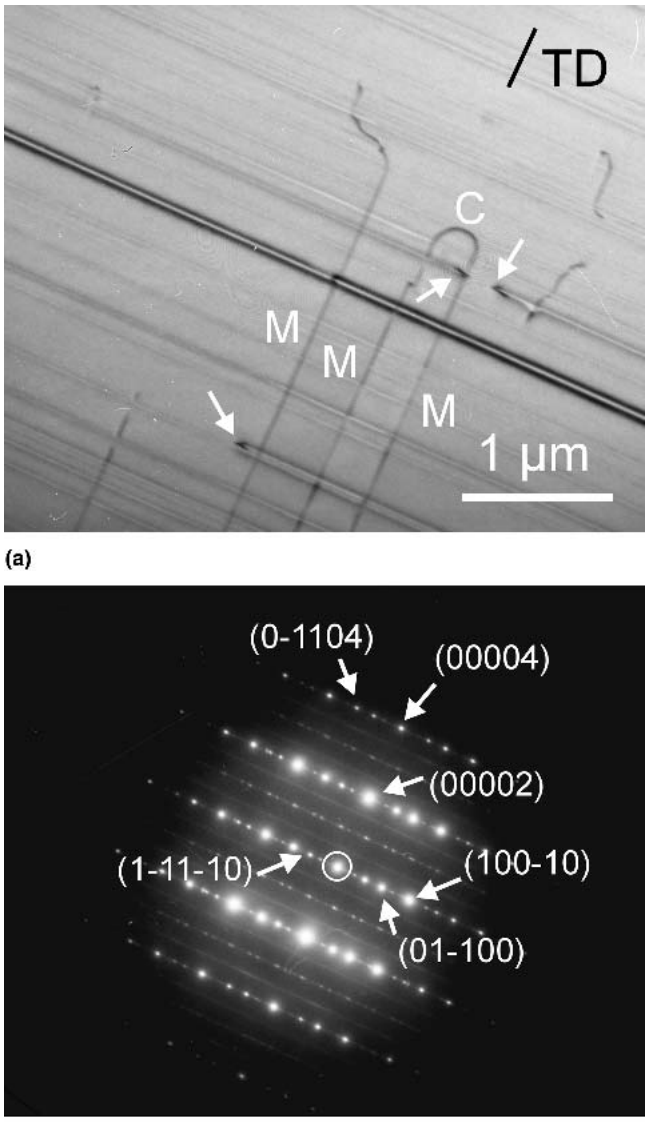

FIG. 1. Typical microstructure during in situ deformation: (a) TEM image and (b) diffraction pattern at the P2 2-fold pole.

diffraction pattern taken at the P2 2-fold pole of the foil normal. Figure 1(a) and most of the other micrographs were taken at this pole with a systematic row of reflections parallel to the periodic axis, i.e., containing the $g = (00002)$ reflection, with a higher reflection excited (high-order bright-field technique). This direction is also the tensile direction (TD). Under these conditions, dislocations with quasiperiodic Burgers vectors are extinguished. The arrows in Fig. 1 point to dislocations with a periodic Burgers vector, which appear as short dark lines that are attached to extended gray lines, which are the traces of the dislocation motion. The periodic dislocations, which are seen almost edge on, move along quasiperiodic planes perpendicular to the periodic axis. Many other traces in the same direction of dislocations which run out of the image area are visible as well. The dark double line in the center of the figure is the trace of many dislocations. The gray lines parallel to the tensile direction, marked by M, are dislocations which, according to Ref. 9, have mixed Burgers vectors.

Figure 2 was taken at a different specimen area with a systematic row containing the quasiperiodic reflection $g = (\bar{1}0010)$. Dislocations with mixed and quasiperiodic Burgers vectors are visible but those with the periodic Burgers vector are now extinguished. The entire image shows a background structure with a striation contrast parallel to the 10-fold axis. Possibly, this contrast originates from phason boundaries resulting from phason disorder.[19] It appears under all diffraction vectors that exhibit any component in the quasiperiodic direction. It makes the observation of dislocations difficult. Therefore, all other micrographs were taken with a diffraction vector parallel to the periodic axis.

B. Dislocation motion

Most dislocations observed moved on planes perpendicular to the periodic axis, as those indicated in Fig. 1 by arrows. These dislocations consist of two straight segments with a sharp knee between them. The orientations of the segments could not be determined since the planes of motion are imaged almost edge-on. These periodic dislocations move by pure climb since their Burgers vector is perpendicular to the plane of motion.[9] As TD is also perpendicular to the plane of motion, the climb force acting on the dislocations from the applied load is maximum and there is no glide force. These dislocations may be called periodic dislocations on the climb system. Sometimes, dislocations of opposite sign move against each other and annihilate, as shown in Fig. 3. In some cases, dislocations move on planes, the traces of which on the specimen surface exhibit the same orientation as those in Fig. 3, but which are inclined with respect to the climb plane. An example is shown in Fig. 4, taken from a video recording where the plane of motion of the

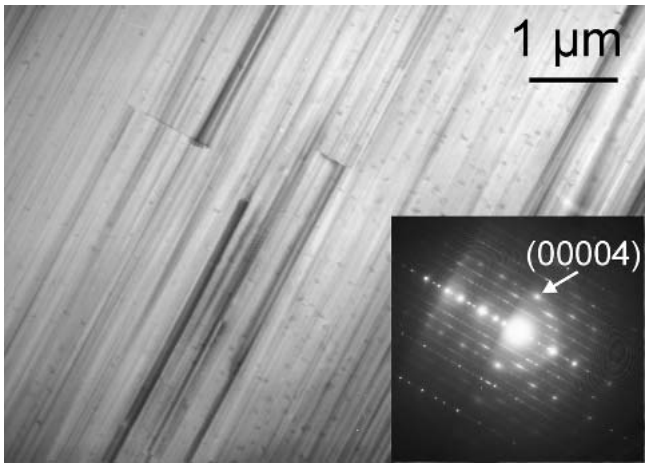

FIG. 2. Microstructure imaged with a systematic row of reflections containing the quasiperiodic reflection $g = (\bar{1}0010)$. (Inset) Respective diffraction pattern.

dislocation marked by the large black arrow changes continuously accompanied with a reduction of the width of the trace labeled by the small white arrows. The motion should then occur by a combination of climb and glide.

Figure 5 demonstrates that dislocations with periodic Burgers vectors may change between the climb plane, labeled *c*, and a plane with a trace inclined with respect to the trace of the climb plane by about 18°, labeled *i*. The places of the transition are marked by black arrows. In Fig. 5, these inclined planes are also imaged edge-on. With reference to the diffraction pattern in Fig. 1(b) (Fig. 5 is slightly rotated against Fig. 1), these planes may be indexed $(0\bar{1}104)$. The mode of motion on these planes is a combination of climb and glide. The inclined trace *i* in the middle of the figure changes into the direction of the Burgers vector or the tensile direction, marked g, and back. The corresponding plane of motion is imaged edge-on, too. It may be indexed $(0\bar{1}100)$. This plane is a glide plane of these dislocations.

A trace of the same type is also shown in the upper left part of the sections of a video recording in Fig. 6. Similar processes are demonstrated at another dislocation iteratively changing its plane of motion. Figure 6(a) presents the dislocation (marked by the white arrow D), which extends approximately perpendicular to the periodic axis (PA), as well as the traces of its previous motion (black arrows). The traces connected directly to the dislocation are parallel to the periodic direction [marked *g* in Fig. 6(b)]. Afterwards, the dislocation shifts to a plane with inclined traces *i* [Figs. 6(b)–6(d)]. In Fig. 6(e), it moves again on the same plane as in Fig. 6(a). In Fig. 6, the planes with the inclined trace *i* and with the trace in the direction of the periodic axis *g* are not imaged edge on. Considering the ratio between the widths of the two traces, the corresponding planes of motion may be indexed $(0\bar{1}002)$ for the inclined trace *i* and (01000) for the

trace *g*. In principle, such a change of planes of motion of a dislocation can be produced by glide and cross glide. The Burgers vector would then be parallel to the intersection line between the two planes, which is parallel to a quasiperiodic direction. These Burgers vectors are, however, extinguished at the present imaging conditions with a *g* vector in the periodic direction. Therefore, it is supposed that the dislocation has also a periodic Burgers vector, since, according to Ref. 9, only these dislocations assume line directions perpendicular to the periodic axis. Thus, the dislocation is a pure edge dislocation. The mode of motion is a combination of climb and glide for the traces *i*, and it is a pure glide motion for the trace *g*. The occurrence of the glide motion is surprising since in the current geometry there should be no glide force in a specimen with a homogeneous cross section. A glide force acting on the dislocation could be due to the inhomogeneous shape of the microtensile specimen. The dislocation velocities measured from the video recording are 1.1 nm s^{-1} for glide in Fig. 6(a), 325 and 285 nm s^{-1} for the combination of climb and glide in Figs. 6(b) and

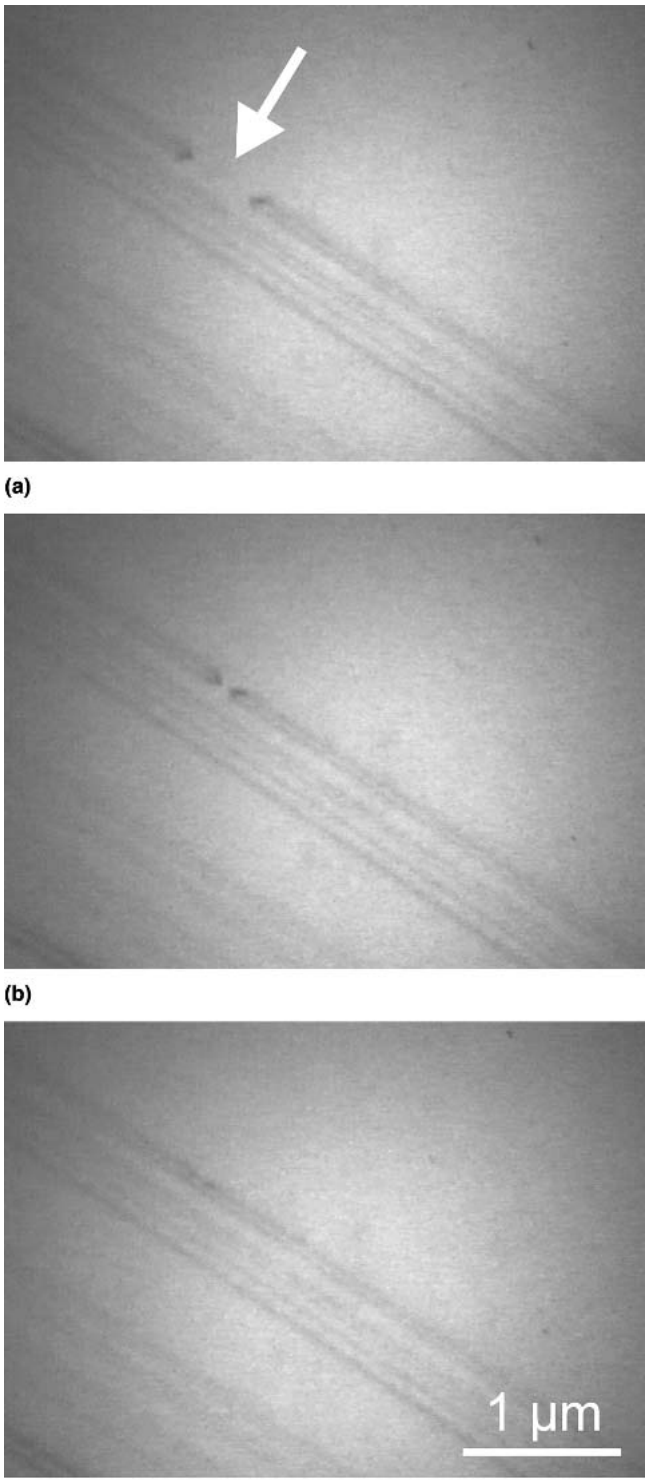

FIG. 3. Annihilation of two periodic dislocations on the climb system.

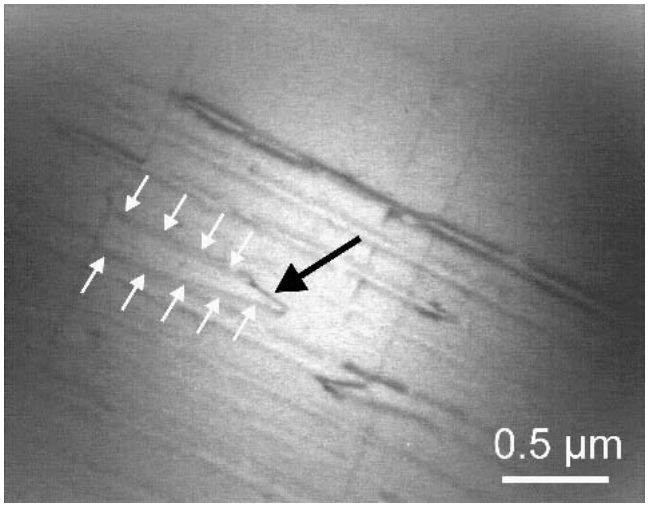

FIG. 4. Video frame of the dislocation movement of periodic dislocations on the climb system as well as of one dislocation changing the plane of motion continuously (arrow).

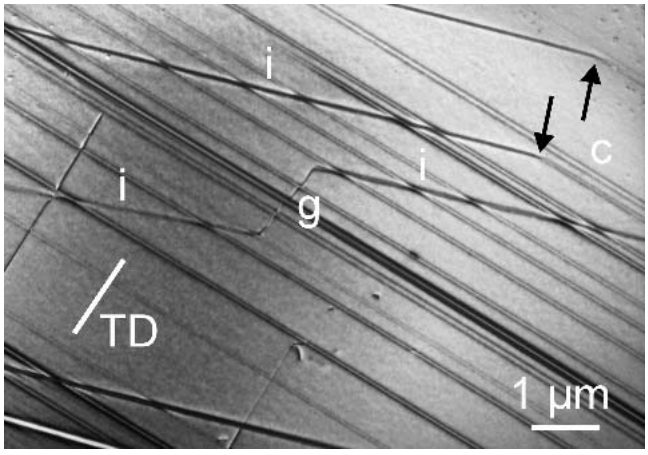

FIG. 5. Micrograph showing traces of periodic dislocations moving on different planes. The inclined planes i may be indexed $(0\bar{1}104)$ and those parallel to the periodic axis g $(01\bar{1}00)$.

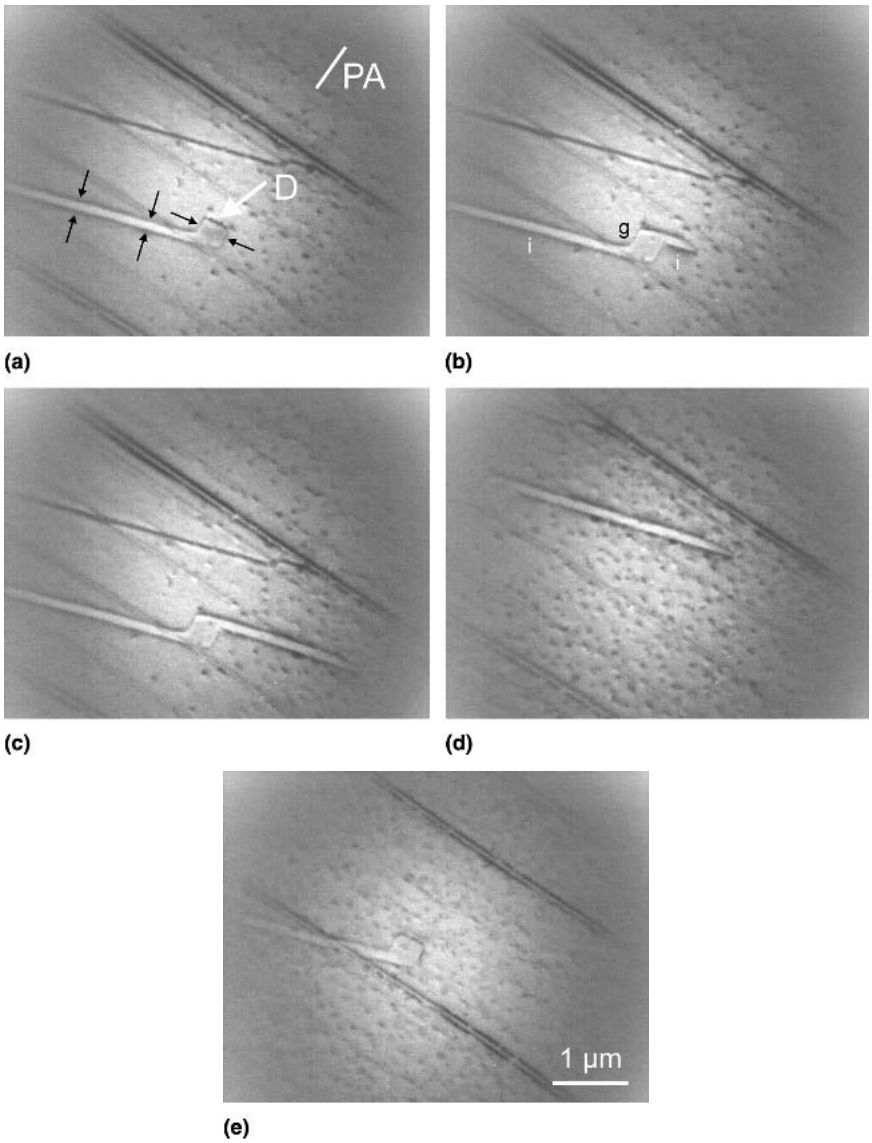

FIG. 6. Sequence from a video recording showing dislocation motion with the transition between different planes of motion. Time: (a) 0 s, (b) 25.5 s, (c) 29.5 s, (d) 33 s, and (e) 83.5 s.

6(d), and 7 nm s^{-1} for glide in Fig. 6(e) and afterwards. In the same specimen area, a dislocation moved on the climb plane with a velocity of 460 nm s^{-1}. While the glide velocity is much smaller than the climb velocity, that by a combination of climb and glide is only slightly lower. Because of the very different acting forces, the relation between the velocities does not describe the relation of the dislocation mobilities on the different planes.

Another set of dislocations are those with mixed Burgers vectors marked M in Fig. 1. They move on planes containing the periodic axis. The dislocation MCM expands by the curved segment C moving upwards thus trailing the long straight dislocations labeled M in Fig. 1. The mode of motion can only be determined by indexing both the plane of motion and the Burgers vector. The determination of the Burgers vector was not possible because of the unsuitable imaging conditions with most *g* vectors (Sec. III. A.). As the plane of motion contains the tensile direction, neither a glide nor a climb force acts on the dislocations from the applied load in a macroscopic sense. Thus, the driving force can only be a chemical force. Dislocation velocities were measured from a video recording which shows a mixed dislocation segment as well as moving periodic dislocations on the climb system. At the same applied stress, the dislocations on the climb system are 20 times faster than the mixed dislocation.

C. Dislocation interaction and multiplication

Dislocations with periodic Burgers vectors can interact with dislocations with mixed Burgers vectors. In most cases, however, the moving periodic dislocations cut the mixed ones without a visible sign of reaction. As pointed

out in Ref. 9, a reaction may happen if the periodic component of the mixed Burgers vector is opposite to the periodic Burgers vector, corresponding to a subtraction of the Burgers vectors B(1) and B(4) of Sec. III. A. The product dislocation has a mixed Burgers vector of the same type with its periodic component of opposite sign. Such an interaction is demonstrated in Fig. 7. In Fig. 7(a), the periodic dislocation P, which exhibits a sharp knee

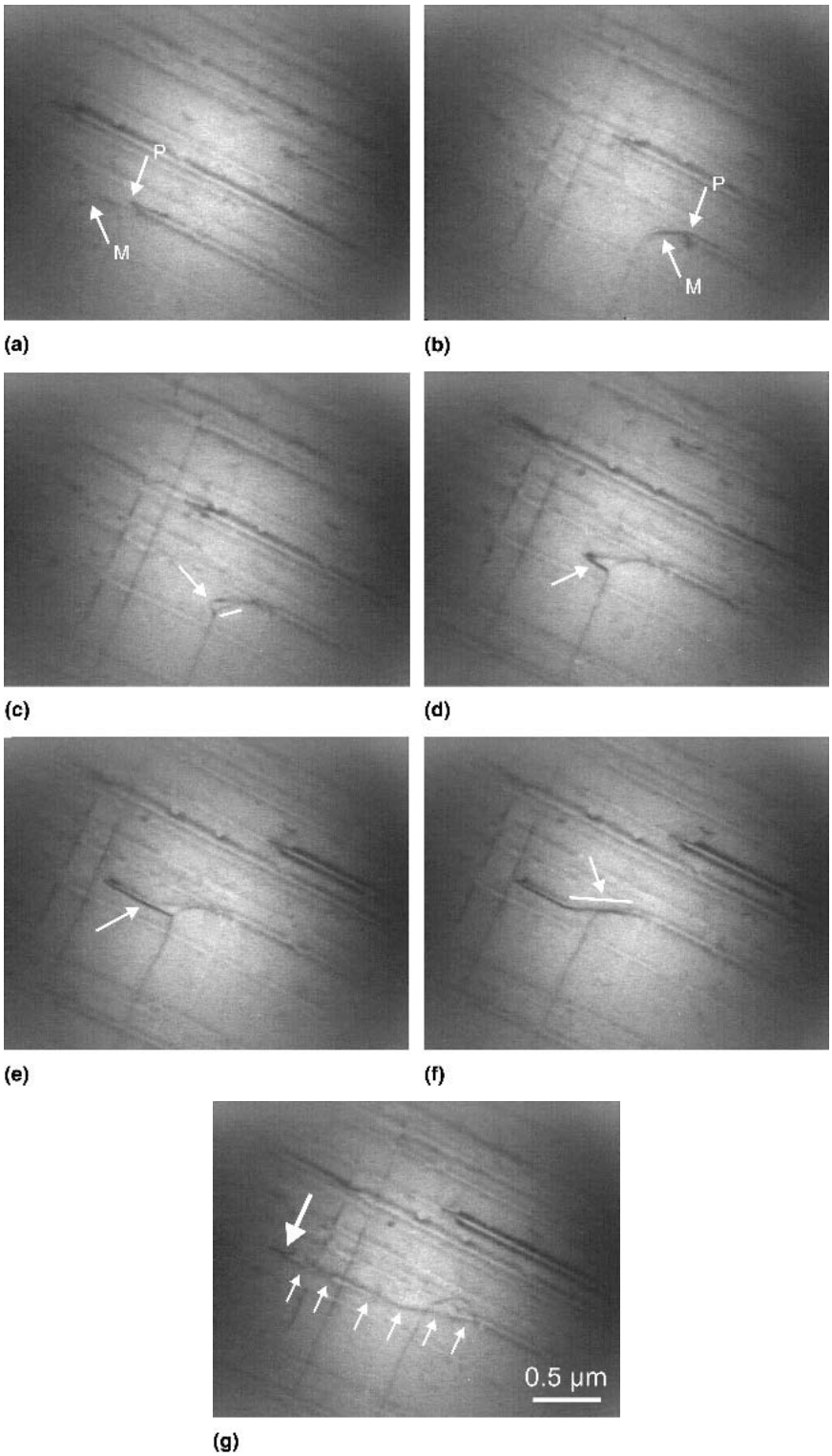

FIG. 7. Sequence from a video recording with the interaction between a dislocation with a periodic Burgers vector P with one with a mixed Burgers vector M. Time: (a) 0 s, (b) 3.6 s, (c) 5.7 s, (d) 32 s, (e) 83.8 s, (f) 88 s, and (g) 104.5 s.

like the dislocations marked by arrows in Fig. 1, moves to the left towards the mixed dislocation M. The mixed dislocation shows a similar curved shape as that in Fig. 1. Both dislocations attract each other and join in Fig. 7(b) to form a segment of the product dislocation, indicated by the white line in Fig. 7(c). At the same time, the climbing periodic dislocation segment (arrow) is shifted onto a parallel climb plane (downwards in the figure) due to the mutual elastic interaction. The latter segment is fixed at the junction with the product dislocation and starts to extend on the new climb plane in Figs. 7(d) to 7(e) (arrow). In Fig. 7(f), the segment indicated by the straight line moves back (upwards in the figure) and removes the product dislocation. As a result, in Fig. 7(g), the mixed dislocation is restored and moves slowly upwards while the periodic dislocation (thick arrow) resumes its motion on the new climb plane. The dark contrasts labeled by the six thin arrows mark the trace of the dislocation motion.

In other cases, the same dislocation reaction results in the formation of a dislocation source, as demonstrated in Fig. 8. In Fig. 8(a), a dislocation with a periodic Burgers vector P moves from right to left close to the bowed part of the dislocation labeled M, which has a mixed Burgers vector. After the mixed dislocation has slowly proceeded upwards, the following periodic dislocation P in Fig. 8(b) reacts with the mixed one to form a junction. Now, however, the segment of the periodic dislocation remains attached to the junction and draws a long dislocation towards the left side [arrows in Figs. 8(c) and 8(d)]. The stages of Figs. 8(c) to 8(f) are schematically drawn in Fig. 8(i). After the new long segment of the periodic dislocation parallel to the specimen surface [arrow in Fig. 8(d)] escaped at the surface, the remaining new dislocation moves out of the image area and the segment attached to the junction rotates to the right side of the mixed dislocation and expands there [arrow in Fig. 8(e)]. In Fig. 8(f), the source has emitted a dislocation moving to the right (arrow pointing upwards) while the rotating arm of the source has turned already to the left side again (arrow pointing downwards). The source continues its revolutions in Figs. 8(g) and 8(h). Figure 8(h) shows both the attached segment of the source extending to the right and a fresh dislocation moving to the left (arrows). After each revolution, the rotating segment shifts slightly down onto a parallel plane. In this way, the generated deformation band grows in width. Several sources of this kind have been observed, emitting tens of dislocations each.

During the observation of one source, the load was changed to study the dynamic dislocation behavior. From the video recordings, the frequency of the revolutions of the source f_{source} was determined as a function of the load F. The results are plotted in Fig. 9(a) in a double-logarithmic scale. Each symbol corresponds to one revolution of the source. During the first part of the experiment, about 30 dislocations were emitted from the source. The frequency of the source decreased only slightly while the load remained almost constant (downward open triangles). Afterwards, the specimen was partly unloaded until the revolution of the source almost stopped. The lowest load was 5.6 N. This phase of the experiment is characterized by a linear decrease of the frequency of the source in the plot of Fig. 9(a) with a load or stress exponent of the frequency of the source $m_{\text{sc ul}} = \text{d ln } (f_{\text{source}})/\text{d ln } F = \text{d ln } (f_{\text{source}})/\text{d ln } \sigma = 7.1$. σ is the flow stress. Afterwards, the specimen was reloaded until fracture (full upward triangles). The figure shows that unloading and reloading is reversible in the lower part of the load range. The reloading curve is linear, too, yielding a stress exponent $m_{\text{sc l}} = 4.4$. At higher loads, the unloading and reloading curves do not coincide. During the reversible part of the experiment, the source emitted only about 10 dislocations. In addition, the velocity v of the dislocations emitted to the left side during reloading was determined from digitized video frames and plotted in Fig. 9(b) also as a function of the load. This curve is linear, too, yielding a load or stress exponent of the dislocation velocity $m' = \text{d ln } \upsilon/\text{d ln } F = \text{d ln } \upsilon/\text{d ln } \sigma$ of 3.9.

IV. DISCUSSION

The present work gives direct evidence of the deformation mechanisms suggested by Schall et al.[9,10,20] for decagonal single quasicrystals loaded parallel to the 10-fold axis. The main mechanism is the climb motion of dislocations with Burgers vectors in the 10-fold periodic direction along the quasiperiodic plane. In the present experiments we observe that these dislocations also move by glide as well as by a combination of climb and glide (Figs. 5 and 6). Assuming homogeneous uniaxial tension along the 10-fold axis, these dislocations do not experience a glide force. In the in situ experiment, however, an inhomogeneous stress field acts with nonvanishing stress components besides the dominating tension along the macroscopic tensile axis.[21] The glide motion of the periodic dislocations was previously observed as the main deformation mechanism at a loading axis inclined by 45° with respect to the 10-fold axis.[9] In addition, we find that the periodic dislocations can also move on well defined crystallographic planes by a combination of climb and glide. This motion is quite unexpected since it is neither defined by the glide plane nor by the plane of maximum stress.

It is pointed out in Ref. 10 that the climb motion of the periodic dislocations experiencing a maximum climb force takes place by a vacancy flux to the mixed dislocations, which experience neither a climb nor a glide force (note that the present specimens are loaded in tension while the macroscopic ones in Ref. 10 are loaded in compression). The latter dislocations move under the

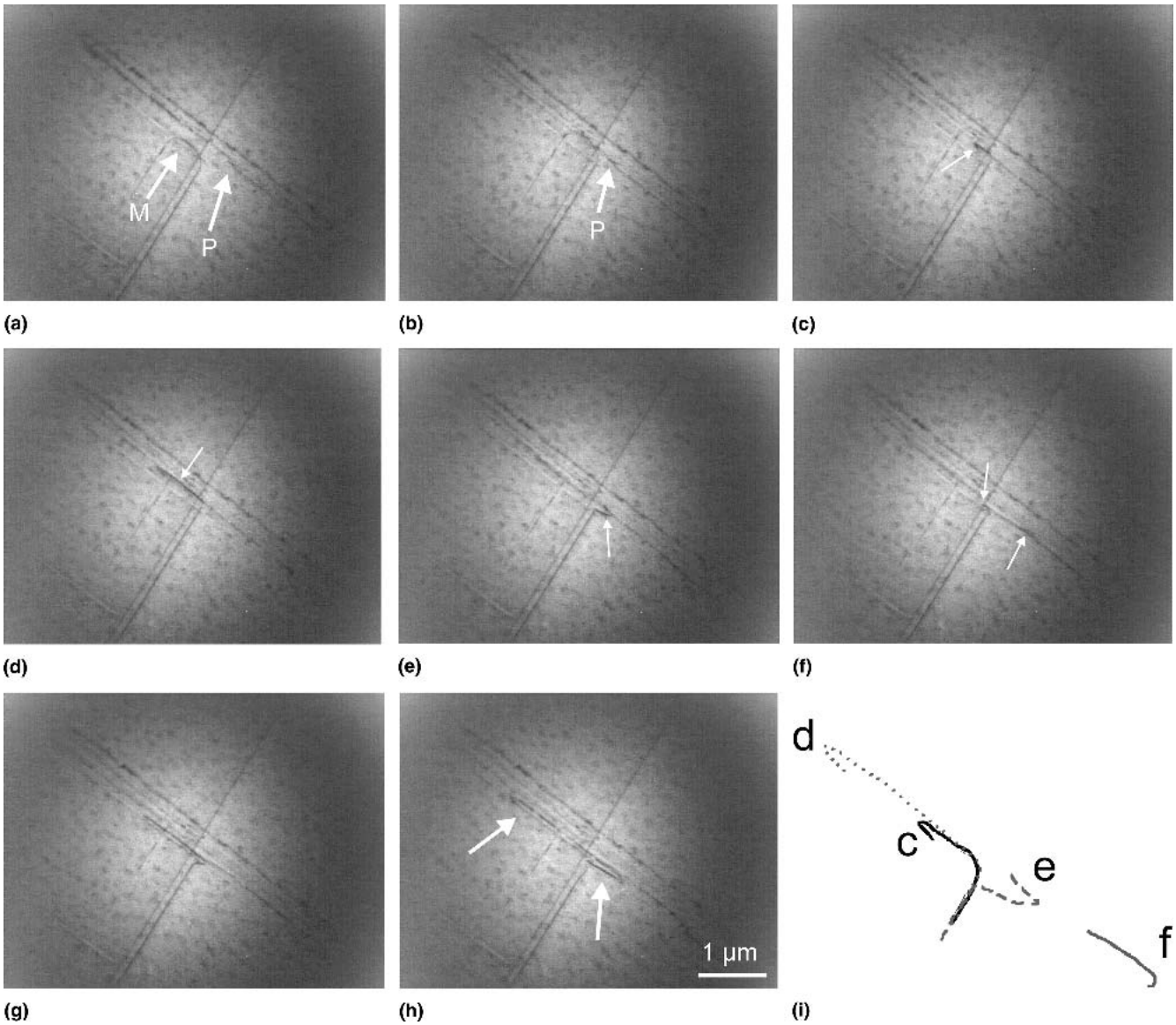

FIG. 8. Video sequence of the formation of a dislocation source by the reaction between a dislocation with a periodic Burgers vector P with one with a mixed Burgers vector M and operation of the source. Time: (a) 0 s, (b) 20.5 s, (c) 25.5 s, (d) 30.5 s, (e) 32.5 s, (f) 35.5 s, (g) 45 s, and (h) 48.5 s.

action of a chemical force resulting from the vacancy supersaturation. In the present experiments, their Burgers vectors have not been explicitly determined, so their mode of motion is not clear.

A situation similar to that of the mixed dislocations is observed in icosahedral quasicrystals where deformation bands are formed with Burgers vectors perpendicular to the compression axis on which neither a climb nor a glide force acts.[16] In bulk material, the mass balance requires that the total flux of vacancies generated by the periodic dislocations is equal to that annihilated at the mixed ones. In the in situ experiments, the few mixed dislocations moved significantly slower than the climbing periodic dislocations, indicating that they do not balance the vacancy flux associated with the climb of the periodic dislocations. In the thin in situ specimens, the close surfaces may act as additional sinks of the excess vacancies which balances the vacancy flux.

Both the periodic as well as the mixed dislocations strictly move on crystallographic planes and exhibit straight crystallographically oriented segments. The strict crystallographic orientation is remarkable and is an important feature of the dislocation motion in the present Al–Ni–Co quasicrystals. This situation is similar to that in icosahedral Al–Pd–Mn quasicrystals, where the dislocations assume straight configurations in the high-temperature range of deformation.[14–16] This straight course does not result from the action of a mechanism connected with the atomic structure similar to the Peierls mechanism in crystals, since this mechanism is a low-temperature mechanism. In Al–Pd–Mn, the dislocations become curved at low temperatures where diffusion is

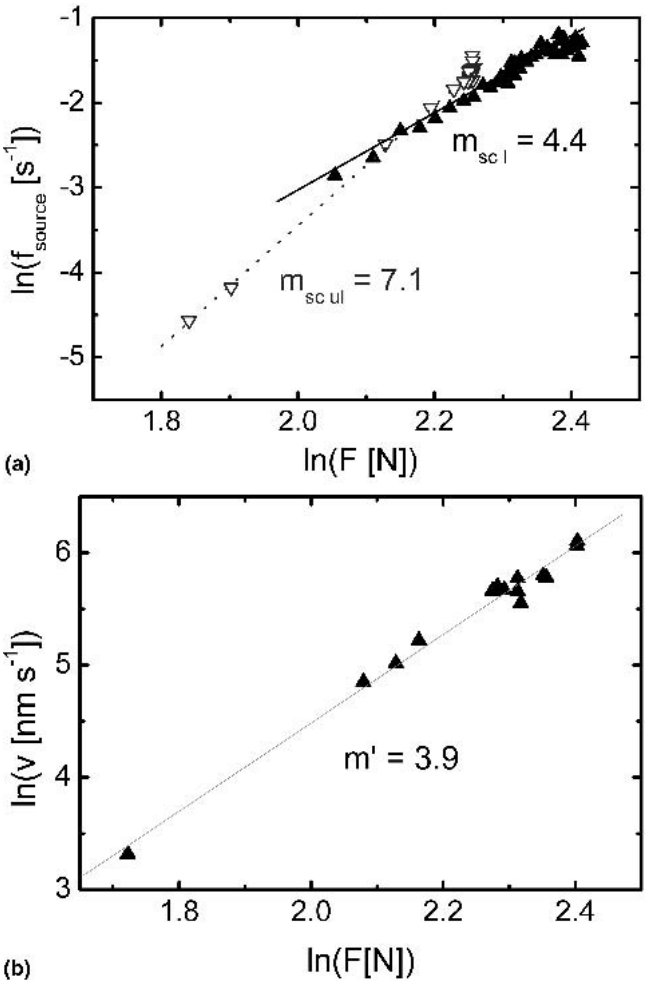

FIG. 9. (a) Load dependence of the frequency of the operation of a dislocation source and (b) velocity of dislocations with periodic Burgers vectors moving away from the source. Open downward triangles: unloading; full upward triangles: re-loading.

not important. It is suggested in Refs. 14 and 15 that both the straight oriented shape and the selection of crystallographic planes of motion other than the glide planes result from special core configurations.

The climb motion of the periodic dislocations in the present tension tests parallel to the periodic axis is similar to some hexagonal metals deformed along the *c* axis at high temperatures. There, the deformation is carried by prismatic dislocation loops with Burgers vectors parallel to the *c* axis.[22,23]

The plastic strain rate resulting from climb of the periodic dislocations can be estimated from the general theory of climb (e.g., Ref. 24). As followed from the activation volume of diffusion, diffusion in icosahedral Al–Pd–Mn takes place by a vacancy mechanism.[25] Internal friction measurements show that this holds also for decagonal quasicrystals.[26] For multicomponent materials, the climb rate is controlled by diffusion of the slowest component. In Al–Ni–Co this is Co. In the case of jogs saturated with vacancies (diffusion controlled climb), the strain rate may be expressed as

$$\dot{\epsilon} = \rho b \upsilon = \frac{\rho b D}{L}\left(\exp\frac{\Omega\sigma}{kT} - 1\right) \quad , \qquad (1)$$

where ρ is the dislocation density, b is the absolute value of the Burgers vector, υ is the dislocation velocity, D is the diffusion coefficient, L is a length characteristic of the diffusion problem, Ω is the atomic volume, k is Boltzmann's constant, and T is the absolute temperature. If it is assumed for simplicity that the diffusion occurs between cylinders of a radius $r = 1/(2\ \rho^{1/2})$ with the dislocations at their centers, then $L = b \ln [r/(2br^{1/2})]$. With values of $b = 0.4$ nm, $\sigma = 330$ MPa,[7] $D_{Co} = 2 \times 10^{-16}$ m^2 s^{-1} at 730 °C,[25] estimated data $\rho = 2 \times 10^{13}$ m^{-2} (density of mixed dislocations in networks with periodic ones[20]), and $\Omega = 1.5 \times 10^{-29}$ m^3, the strain rate becomes 7×10^{-4} s^{-1}. This is about two orders of magnitude greater than the strain rate of the macroscopic experiments.[7] Thus, climb should be fast enough to explain the macroscopic deformation rates.

The stress exponents following from the dislocation mobility measured in the present study (Fig. 9) and the macroscopic deformation data from Ref. 7, however, do not fit climb-controlled deformation. Dislocation mobility data obtained from in situ straining tests have to be considered with some care because of the inhomogeneous stress field in the microtensile specimens. As calculated in Ref. 21 for an elastically strained in situ specimen, the regions at the side edges of the perforation experience almost a uniaxial tensile stress of about three times the macroscopic average stress like the result of the engineering mechanics treatment of a plate with a hole. In the present experiments, the observations were made at a fixed place of a dislocation source so that the geometry did not change during the measurements. Because of the plastic deformation during the load change experiment, however, dislocations are stored, resulting in a change of the internal stress. This effect leads to the initial decrease of the frequency of the source at almost constant load [upper frequency values of the unloading curve in Fig. 9(a)]. Similarly, during reloading, a higher load is necessary to reach the same frequencies as during unloading in the high-frequency range. However, in the low-load range where only about 10 dislocations were emitted, the dependence of the frequency of the source depends almost reversibly on the load [Fig. 9(a)], showing that the internal stress did not change in this range, i.e., the specimen behaves almost elastically. The scaling factor between the load on the specimen and the local applied stress does not enter the determination of the stress exponent. Thus, the data in Fig. 9 should give reliable values of the stress exponent m'.

The relevant quantity describing the dislocation dynamics is the (true) stress exponent $m = \mathrm{d}\ln v/\mathrm{d}\ln\sigma^* = \mathrm{d}\ln\dot{\epsilon}/\mathrm{d}\ln\sigma^*$ (if the mobile dislocation density is constant during the test). Here, σ^* is the effective stress, which is the difference between the total flow stress σ and the internal stress component σ_i, $\sigma^* = \sigma - \sigma_i$. In all experiments, the stress exponent $m' = \mathrm{d}\ln v/\mathrm{d}\ln\sigma = \mathrm{d}\ln\dot{\epsilon}/\mathrm{d}\ln\sigma$ is measured instead of m. Both may deviate substantially from each other because of the internal stress component σ_i. In the present experiments, the load dependence of the frequency of the dislocation source as well as the load dependence of the dislocation velocity yield m' values between about 7 and 4. In the macroscopic experiments presented in Refs. 6, 7, and 27 the stress exponents range between $m' \approx 10$ for $Al_{73}Ni_{10}Co_{17}$ and $m' \approx 6$ for $Al_{70}Ni_{15}Co_{15}$. For climb-controlled motion, however, a (true) stress exponent m equal to unity is expected. In the macroscopic experiments, a high density of dislocations in networks was observed. The authors of Ref. 27 estimate the internal stress in the dislocation networks to be of the same order of magnitude as the applied stress and argue that, therefore, the measured stress exponent m' may be substantially greater than the true one m.

For the in situ experiments, the internal stress component is difficult to estimate. The density of mixed dislocations is much lower, most likely due to the close surfaces of the in situ samples, which act as additional sinks of vacancies. The dislocations usually cut each other without a sign of reaction. For the moving periodic dislocations, there should act a back stress from the other dislocations emitted from the source. At the minimum of the load change test, the dislocations moved still very slowly at a load of 5.6 N. It may therefore be assumed that the internal load component is 5 N at maximum. Regression analysis of the data of Fig. 9 with the load reduced by 5 N yields stress exponents of 2.35 for unloading and 2.1 for loading. Thus, the true stress exponent may be slightly greater than 2. The deviation of this value from unity suggests that other mechanisms than climb control the dislocation mobility. As in icosahedral quasicrystals, these mechanisms may be connected with the cluster structure. For icosahedral quasicrystals stress exponents of around 5 have been determined. For these materials, the macroscopic deformation data can well be interpreted by models of cluster friction,[28] considering that the clusters are overcome in a collective way[29] or by a Peierls mechanism on the cluster scale.[30] The latter interpretation was applied to decagonal Al–Ni–Co already in Refs. 3 and 20. Instead of the clusters in icosahedral quasicrystals, the pentagonal antiprismatic channels[18] building up the structure may act as the obstacles to dislocation motion. These structures have to be cut by both the climb motion of dislocations with periodic Burgers vectors and by glide or climb of dislocations with quasicrystalline or mixed Burgers vectors.

V. CONCLUSION

The following conclusions hold for decagonal Al–Ni–Co deformed along the 10-fold periodic axis.

For the first time, the climb, glide and combined climb and glide motion of dislocations with Burgers vectors in the periodic direction have directly been observed. Dislocation velocities were measured for the different modes of motion.

Dislocations with mixed Burgers vectors move on planes where no (or, because of the special specimen geometry, only a small) force acts, i.e., under the action of a chemical force. These observations support the deformation model established by Schall et al.

The dislocations are arranged along crystallographic directions, and they move on well-defined crystallographic planes. This may be interpreted by a particular core structure.

The deviation of the measured stress exponent of the dislocation velocity from the stress exponent for climb suggests that the dislocation mobility is controlled by other mechanisms, which may be due to the structure of decagonal quasicrystals consisting of decagonal antiprismatic channels.

ACKNOWLEDGMENTS

The authors are grateful for the support of the work by Professors J. Kirschner and K. Urban. They acknowledge technical help by Rosamunde Möhner and Christian Dietzsch.

REFERENCES

1. M. Wollgarten, M. Beyss, K. Urban, H. Liebertz, and U. Köster: Direct evidence of plastic deformation of quasicrystals by means of a dislocation mechanism. *Phys. Rev. Lett.* **71,** 549 (1993).
2. M. Wollgarten, M. Bartsch, U. Messerschmidt, M. Feuerbacher, R. Rosenfeld, M. Beyss, and K. Urban: In-situ observation of dislocation motion in icosahedral Al–Pd–Mn single quasicrystals. *Philos. Mag. Lett.* **71,** 99 (1995).
3. M. Feuerbacher, M. Bartsch, G. Grushko, U. Messerschmidt, and K. Urban: Plastic deformation of decagonal Al–Ni–Co quasicrystals. *Philos. Mag. Lett.* **76,** 369 (1997).
4. K. Edagawa, Y. Arai, T. Hashimoto, and S. Takeuchi: Plastic anisotropy in an Al–Cu–Co decagonal quasicrystals. *Mater. Trans. JIM* **39,** 863 (1998).
5. K. Edagawa, S. Ohta, S. Takeuchi, E. Kabutoya, J.Q. Guo, and A-P. Tsai: Plasticity of Al–Ni–Co decagonal single quasicrystals. *Mater. Sci. Eng. A* **294–296,** 748 (2000).
6. P. Schall, M. Feuerbacher, and K. Urban: Plastic deformation behaviour of decagonal $Al_{70}Ni_{15}Co_{15}$ single quasicrystals. *Philos. Mag. Lett.* **81,** 339 (2001).
7. P. Schall, M. Feuerbacher, and K. Urban: Plastic deformation of

decagonal $Al_{37}Ni_{10}Co_{17}$ single quasicrystals. *Philos. Mag.* **84,** 705 (2004).
8. Z. Zhang and K. Urban: Transmission electron-microscope observation of dislocations and stacking faults in a decagonal Al–Cu–Co alloy. *Philos. Mag. Lett.* **60,** 97 (1989).
9. P. Schall, M. Feuerbacher, and K. Urban: Dislocations and dislocation reactions in decagonal Al–Ni–Co quasicrystals. *Phys. Rev. B.* **69,** 134105 (2004).
10. P. Schall, M. Feuerbacher, and K. Urban: Plasticity of decogonal $Al_{37}Ni_{10}Co_{17}$ quasicrystals, in *Quasicrystals 2003—Preparation, Properties and Applications*, edited by E. Belin-Ferré, M. Feuerbacher, Y Ishii, and D.J. Sordelet (Mater. Res. Soc. Symp. Proc. **805,** Warrendale, PA, 2004), LL 5.5, p. 175.
11. D. Caillard, F. Mompiou, L. Bresson, and D. Gratias: Dislocation climb in icosahedral quasicrystals. *Scripta Mater.* **49,** 11 (2003).
12. F. Mompiou, D. Caillard, and M. Feuerbacher: In-situ observation of dislocation motion in icosahedral Al–Pd–Mn quasicrystals. *Philos. Mag.* **84,** 2777 (2004).
13. F. Mompiou, L. Bresson, P. Cordier, and D. Caillard: Dislocation climb and low-temperature plasticity of an Al–Pd–Mn quasicrystal. *Philos. Mag.* **83,** 3133 (2003).
14. U. Messerschmidt, M. Bartsch, B. Geyer, and L. Ledig: in *Quasicrystals, Structure and Physical Properties*, edited by H-R. Trebin (Wiley-VCH, Weinheim, Germany, 2003), p. 462.
15. U. Messerschmidt and M. Bartsch: Mechanisms of plastic deformation of icosahedral quasicrystals. *Scripta Mater.* **49,** 33 (2003).
16. U. Messerschmidt, L. Ledig, and M. Bartsch: Temperature dependence of dislocation processes during plastic deformation of i-Al–Pd–Mn single quasicrystals. *J. Non-Cryst. Solids* **334,** 436 (2004).
17. U. Messerschmidt and M. Bartsch: High-temperature straining stage for in situ experiments in the high-voltage electron microscope. *Ultramicroscopy* **56,** 163 (1994).
18. W. Steurer, T. Haibach, B. Zhang, S. Kek, and R. Lück: The structure of decagonal $Al_{70}Ni_{15}Co_{15}$. *Acta Crystallogr. Sect. B: Struct. Sci.* **49,** 661 (1993).
19. N.K. Mukhopadhyay, G.C. Weatherly, and G.V.S. Sastry: On the analysis of diffuse intensity and striation contrast in electron microscopy images of Al–Cu–Co–Si decagonal phases. *Mater. Sci. Eng. A* **294–296,** 135 (2000).
20. M. Feuerbacher and P. Schall: Plastic behaviour of decagonal Al–Ni–Co single quasicrystals. *Scripta Mater.* **49,** 25 (2003).
21. A. Coujou, P. Lours, N.A. Roy, D. Caillard, and N. Clement: Determination of the local tensile axis direction in a TEM in situ strained γ'-single crystals—A finite element approach. *Acta Metall. Mater.* **38,** 825 (1990).
22. J.F. Stohr and J.P. Poirier: Electron-microscope study of pyramidal slip [1122] [1123] in magnesium. *Philos. Mag.* **25,** 1313 (1972).
23. G. Edelin and J.P. Poirier: Study of dislocation climb by means of diffusional creep experiments in magnesium. 1. Deformation mechanism. *Philos. Mag.* **28,** 1203 (1973).
24. J. Friedel: *Dislocations* (Pergamon Press, Oxford, U.K., 1964).
25. H. Mehrer and R. Galler: Vacancy-mediated diffusion in quasicrystalline alloys. *J. Alloys Compd.* **342,** 296 (2002).
26. M. Weller, B. Damson, and M. Feuerbacher: Defects and diffusion in d-AlNiCo-quasicrystals—Application of mechanical spectroscopy. (unpublished, 2004).
27. P. Schall, M. Feuerbacher, and K. Urban: Plasticity of decagonal Al–Ni–Co quasicrystals (unpublished).
28. M. Feuerbacher, C. Metzmacher, M. Wollgarten, K. Urban, B. Baufeld, M. Bartsch, and U. Messerschmidt: The plasticity of icosahedral quasicrystals. *Mater. Sci. Eng. A* **233,** 103 (1997).
29. U. Messerschmidt, M. Bartsch, M. Feuerbacher, B. Geyer, and K. Urban: Friction mechanism of dislocation motion in icosahedral Al–Pd–Mn quasicrystals. *Philos. Mag. A* **79,** 2123 (1999).
30. U. Messerschmidt, D. Häussler, M. Bartsch, B. Geyer, M. Feuerbacher, and K. Urban: Microprocesses of the plastic deformation of icosahedral Al–Pd–Mn single quasicrystals. *Mater. Sci. Eng. A* **294–296,** 757 (2000).